Ohtsuka, E., Doi, T., Fukumoto, R., Matsugi, J., & Ikehara, M. (1983) *Nucleic Acids Res. 11*, 3863–3872.
Rich, A. R., & RajBhandary, U. L. (1976) *Annu. Rev. Biochem. 45*, 805–860.
Schulmann, L. H., & Pelka, H. (1983) *Proc. Natl. Acad. Sci. U.S.A. 80*, 6755–6759.
Schulmann, L. H., Pelka, H., & Susani, M. (1983) *Nucleic Acids Res. 11*, 1439–1455.
Seong, B. L., & RajBhandary, U. L. (1987) *Proc. Natl. Acad. Sci. U.S.A. 84*, 8859–8863.
Shibahara, S., Mukai, S., Nishimura, T., Inoue, H., Ohtsuka, E., & Morisawa, H. (1987) *Nucleic Acids Res. 15*, 4403–4415.
Stepanova, O. B., Metelev, V. G., Chichkova, N. V., Smirnov, V. P., Rochionova, N. P., Atabekov, J. G., Bogdanor, A. A., & Shabarova, Z. A. (1979) *FEBS Lett. 103*, 197–199.
Uemura, H., Imai, M., Ohtsuka, E., Ikehara, M., & Soll, D. (1982) *Nucleic Acids Res. 10*, 6531–6539.
Zang, A. J., Been, M. D., & Cech, T. R. (1986) *Nature 324*, 429–433.

Comparative Proton NMR Analysis of Wild-Type Cytochrome *c* Peroxidase from Yeast, the Recombinant Enzyme from *Escherichia coli*, and an Asp-235 → Asn-235 Mutant†

James D. Satterlee*
Department of Chemistry, Washington State University, Pullman, Washington 99164-4630, and Department of Chemistry, University of New Mexico, Albuquerque, New Mexico 87131
James E. Erman
Department of Chemsitry, Northern Illinois University, DeKalb, Illinois 60115
J. Matthew Mauro‡ and Joseph Kraut
Department of Chemistry, University of California, San Diego, La Jolla, California 92093
Received March 1, 1990; Revised Manuscript Received April 27, 1990

ABSTRACT: Proton NMR spectra of cytochrome *c* peroxidase (CcP) isolated from yeast (wild type) and two *Escherichia coli* expressed proteins, the parent expressed protein [CcP(MI)] and the site-directed mutant CcP(MI,D235N) (Asp-235 → Asn-235), have been examined. At neutral pH and in the presence of only potassium phosphate buffer and potassium nitrate, wild-type Ccp and CcP(MI) demonstrate nearly identical spectra corresponding to normal (i.e., "unaged") high-spin ferric peroxidase. In contrast, the mutant protein displays a spectrum characteristic of a low-spin form, probably a result of hydroxide ligation. Asp-235 is hydrogen-bonded to the proximal heme ligand, His-175. Changing Asp-235 to Asn results in alteration of the p*K* for formation of the basic form of CcP. Thus, changes in proximal side structure mediate the chemistry of the distal ligand binding site. All three proteins bind F^-, N_3^-, and CN^- ions, although the affinity of the mutant protein (D235N) for fluoride ion appears to be much higher than that of the other two proteins. Analysis of proton NMR spectra of the cyanide ligated forms leads to the conclusion that the mutant protein (D235N) possesses a more neutral proximal histidine imidazole ring than does either wild-type CcP or CcP(MI). It confirms that an important feature of the cytochrome *c* peroxidase structure is at least partial, and probably full, imidazolate character for the proximal histidine (His-175).

Yeast cytochrome *c* peroxidase (CcP; EC 1.11.1.5) is the most thoroughly characterized of the heme peroxidases. It is a medium-sized (M_r = 34K) ferriheme enzyme that is paramagnetic in its high-spin (resting state, native) and low-spin (ligated) forms. This heme-centered paramagnetism acts as an intrinsic shift and relaxation agent that facilitates proton NMR studies of the heme and its neighboring amino acids in the enzyme's active site (La Mar, 1979; Satterlee, 1986).

Elucidating specific structural features of CcP that imbue it with its characteristic chemistry and differentiate it from other classes of heme proteins has long been a goal (Finzel et al., 1984). On the basis of the refined wild-type CcP structure (Finzel et al., 1984), it was proposed that a hydrogen bond between His-175 N_δ (the proximal histidine bonded to heme iron) and Asp-235 occurs (Figure 1A). Circumstantial support for this type of proximal effect comes from experimental evidence involving other heme proteins (Peisach, 1975), horseradish peroxidase (HRP; de Ropp et al., 1985), and heme models (Traylor & Popvitz-Biro, 1988). The results from horseradish peroxidase are especially pertinent because, like CcP, HRP has oxidized intermediates that are low-spin ferryl species. The NMR results for HRP (de Ropp et al., 1985) clearly showed that full deprotonation of the proximal histidine (Figure 1C) occurs for low-spin, cyanide-ligated HRP (HRP-CN). Those results imply similar proximal imidazolate

† We gratefully acknowledge the following agencies for their support of this work: the National Institutes of Health (DK 30912 and HL 01758, Research Career Development Award) and the National Science Foundation (DMB 8716511 to J.D.S., DMB 8511656 to J.K., and DMB 8716459 to J.E.E.).
* Address correspondence to this author at Washington State University.
‡ Present address: Center for Advanced Research in Biotechnology, 9600 Gudelsky Dr., Rockville, MD 20850.

0006-2960/90/0429-8797$02.50/0

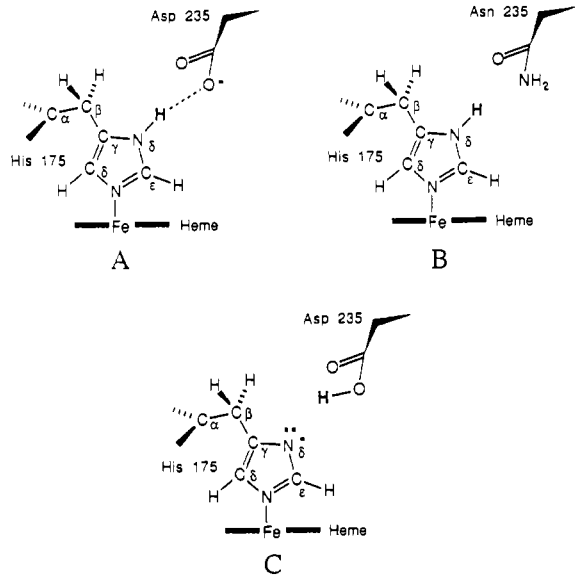

FIGURE 1: Representation of the heme group with the coordinated proximal histidine (His-175) and Asp-235, as in wild-type native CcP and CcP(MI), or Asn-235, as in the mutant CcP(MI,D235N). Various possible protonation states related to the hydrogen bonding between residue 175 and residue 235 are depicted.

structures for the low-spin intermediates, HRP-I and HRP-II.

In order to provide additional experimental evidence about the state of proximal histidine protonation in peroxidases, to explore the question of proximal mediation of heme chemistry, and to demonstrate the integration of site-directed mutagenesis with NMR spectroscopy, we have undertaken a comparative proton NMR study of wild-type yeast CcP, a recombinant yeast CcP expressed in *Escherichia coli* [CcP(MI)] (Fishel et al., 1987), and a site-directed mutant of CcP(MI) in which Asp-235 is replaced by Asn [CcP(MI,D235N), simply abbreviated D235N (Figure 1B)]. Simultaneously, X-ray diffraction data for CcP(MI) and three mutant proteins, including D235N, have been acquired (Wang et al., 1990). That work has resulted in solid-state structural comparisons between wild-type CcP and CcP(MI) that indicate virtually indentical structures for the two proteins. Structural contrasts between CcP(MI) and CcP(MI,D235N) were also carried out in that work, so that there is an independent basis for evaluation the results derived from NMR studies.

If hydrogen bonding involving His-175 is critical for regulating the heme chemistry in CcP, the Asp-235 → Asn-235 mutation would, a priori, be expected to alter the extent of such hydrogen bonding in comparison to that of wild-type CcP or CcP(MI). This mutation should effect detectable changes in NMR spectra of the mutant protein, D235N, compared to those of wild-type native yeast CcP and CcP(MI). Our results show that this mutation does have remarkable proton NMR manifestations and substantiate the importance of proximal hydrogen bonding in CcP.

Experimental Procedures

Native (wild-type) CcP from bakers's yeast (Red Star, Milwaukee, WI) was isolated and purified as previously described (Satterlee & Erman, 1980). The preparation used in this study had a purity index (A_{408nm}/A_{280nm}) of 1.27. The *E. coli* expressed native protein [CcP(MI)] and the D235N mutant were isolated as before (Fishel et al., 1987) and prepared for NMR studies directly from frozen crystals. The *E. coli* expressed native protein [CcP(MI)] contains two primary sequence differences compared to our wild-type native CcP: Asp-152 → Gly and Thr-53 → Ile.

Evidence presented here suggests that both the CcP(MI) and D235N mutant preparations examined by NMR have minor levels (10–25%) of magnetically distinct forms. Prior to NMR analysis SDS–PAGE was carried out with 14% gels. Gels of our preparations of CcP(MI) and D235N displayed single bands, each migrating at ca. 34K. Furthermore, both CcP(MI) and D235N crystallized and were used to obtain X-ray structures (Wang et al., 1990). These results are considered good evidence that our preparations are homogeneous in terms of protein content.

Proton NMR spectra were obtained on a GE360 spectrometer operating at 361 MHz using methods previously described (Satterlee & Erman, 1980; Satterlee et al., 1983). Frozen crystalline samples of each protein were dissolved in a buffer consisting of 260 mM KNO_3 and 40 mM potassium phosphate in 99.9% D_2O (Isotec). They were concentrated on an Amicon stirred pressure cell, rediluted with the buffer, and then reconcentrated. This cycle was repreated at least three times. The final protein concentrations were 2.0–2.4 mM. Proton spectral shifts are reported relative to the residual (HDO) peak (4.63 ppm). Adjustment of solution pH was made by using solutions of DCl or NaOD (Merck) in 99.9% D_2O (Isotec) and measuring with a Beckman pHi 60 meter and calibrated combination electrode. Reported pH values for D_2O/NMR solutions are uncorrected for deuterium isotope effect and are reported as pD.

The variable percent H experiments shown in Figure 5 were carried out beginning with a protein sample in the 99.9% D_2O buffer described above (0.1% H solution). Following that spectrum the sample was diluted 20-fold with a buffer solution made 50% v/v H_2O/D_2O and concentrated by pressure ultrafiltration. This cycle was repeated four times total. After the 50% H spectrum shown in Figure 5B was obtained, an identical set of dilution/reconcentration ultrafiltration cycles was performed with a buffer made 95% v/v H_2O/D_2O. Deionized, glass-distilled H_2O was used in these experiments.

Results and Discussion

Unligated Proteins. (A) Proton Spectra. The consequences of introducing the mutation Asp-235 → Asn are dramatic, as shown by Figure 2, which provides examples of the proton spectra of native wild-type yeast CcP (A), CcP(MI) (B), and the mutant protein CcP(MI,D235N) (C), all obtained under identical conditions. For the D235N mutant (Figure 2C) the entire spectrum is shown, with insets consisting of vertical expansions of the downfield (90–10 ppm) and upfield (−4 to −20 ppm) isotropic shift regions. In the interest of conciseness only the downfield and upfield isotropic shift regions are shown for CcP(MI) and wild-type CcP because these regions are the ones upon which most of the following analysis is based. Comparisons of specific resonance positions for the three proteins and assignments for CcP are given in Table I. The precise resonance positions are not identical, which is probably a consequence of two strain-specific primary sequence differences between our native wild-type CcP and CcP(MI): Asp-152 → Gly and Thr-53 → Ile (Fishel et al., 1987). It has been demonstrated that these sequence differences result in slight structural differences in crystalline CcP(MI), primarily around His-52, compared to crystalline native CcP (Wang et al., 1990), and this slight structural difference may cause the minor shift differences between wild-type and expressed native proteins.

Native wild-type CcP (Figure 2A) and CcP(MI) (Figure 2B) exhibit very similar spectra under these conditions, whereas the spectrum of CcP(MI,D235N) (Figure 2C) is dramatically different, most notably in the range of shifts

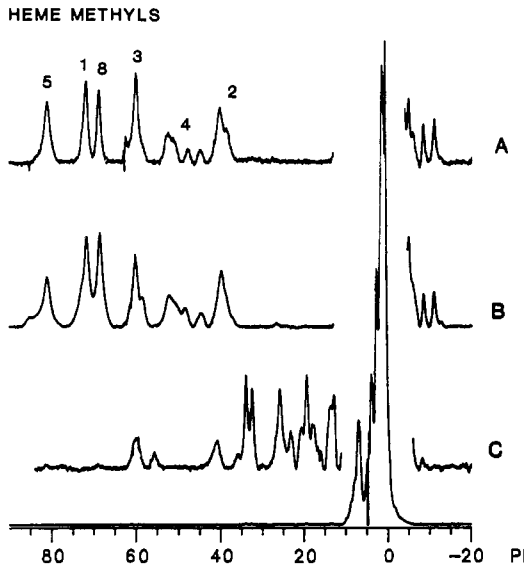

FIGURE 2: Proton NMR spectrum (361 MHz) of the downfield and upfield hyperfine shift regions of (A) wild-type native CcP isolated from yeast, (B) CcP(MI), and (C) the mutant protein CcP(MI,D235N). (C) also shows the complete proton spectrum for D235N at smaller vertical expansion. Assignments shown are definite only for wild-type native CcP. Assignment labels 2 and 4 refer to the α protons of the heme vinyl groups. Solution conditions were 0.2 M KNO_3 and 0.05 M potassium phosphate, pD 6.8 ± 0.2, and 22 ± 2 °C. An rf noise spike artifact occurs near 60 ppm in (A) and (B).

exhibited. The wild-type CcP spectrum in Figure 2A is typical of a high-spin ferriheme protein. The resonances are labeled with proton assignments made previously (Satterlee et al., 1983a). Differences in the D235N spectrum are apparent in both the 0–10 ppm shift region (data not shown) and the isotropic shift region (Figure 2). The existing body of data on proton NMR of ferric heme complexes (La Mar & Walker, 1979) and ferriheme proteins (La Mar, 1979; Satterlee, 1986) provides a basis for interpreting these differences. Wild-type Ccp and CcP(MI) display broader resonances and larger downfield shifts, which are expected for ferriheme proteins in largely high-spin orbital ground states (La Mar, 1979; Satterlee, 1986). CcP(MI,D235N) (Figure 2C) exhibits a smaller range of shifts in the downfield hyperfine shift region (60–10 ppm) with major downfield resonances that do not exceed 40 ppm. The smaller shift range and narrower line widths of the major resonances are indicative of a predominantly low-spin, six-coordinate ferriheme protein.

Contributing to this conclusion is the similarity of the D235N spectrum to that of azide-ligated wild-type CcP (Satterlee et al., 1983b), the the azide-ligated D235N spectrum, and to the cyanide-ligated forms of each (vide infra). Furthermore, the range of shifts for the most downfield resonances in Figure 2C is remarkably similar to the spectrum of metmyoglobin–OH, a six-coordinate, low-spin ferric protein (McGrath & La Mar, 1978). The shift comparison of azide-ligated and hydroxy-ligated ferriheme proteins given in Table II illustrates these similarities.

Two conclusions may be drawn from this comparison. First, the spectra of wild-type CcP and CcP(MI) are nearly identical, leading us to conclude that the assignments made for wild-type native CcP are equally valid for CcP(MI). Second, the set of major resonances of CcP(MI,D235N) represent a predominantly low-spin six-coordinate protein form. On the basis of results presented later and the similarity of the D235N spectrum to that of metmyoglobin–OH (McGrath & La Mar, 1978; La Mar et al., 1980; Krishnamoorthi et al., 1984), we assign hydroxide ion as the sixth ligand for the major form

Table I: Observed Proton Hyperfine Shifts (ppm) in Wild-Type Native CcP, CcP(MI), and CcP(MI,D235N)[a]

assignment in CcP	CcP	CcP(MI)	CcP(MI,D235N)
heme 5-CH_3	80.98	81.13	
heme 1-CH_3	71.76	71.69	
heme 8-CH_3	68.67	68.50	
heme 3-CH_3	60.00	60.19	
		58.62 sh	59.72
	52.34	52.05	55.80
	51.14	50.65	52.39
heme 4α	47.71	48.33	
	44.81	44.52	
	40.07	39.83	40.89
heme 2α	38.45	(39.83)	
			35.73 sh
			33.97
			32.47
			29.86
			26.55 sh
			25.85
			23.14
			20.78
			19.40
			17.73
			15.90
			13.65 br
			12.86 br
	11.51	11.50	
	10.61	10.63	
			9.72
			8.61
	−1.73	−1.80	−1.79
	−2.61	−2.69	
	−3.03	−2.93 sh	
			−3.52
			−4.35
	−5.06	−4.96	−5.10
	−6.35	−6.39	
heme 4β	−8.60	−8.58	−8.34
heme 2β	−11.14	−11.02	

[a] Taken at 21 °C in 260 mM KNO_3 and 40 mM potassium phosphate, pD 6.9 ± 0.1; referenced to internal HDO assigned 4.63 ppm; sh indicates unresolved shoulder; br indicates broad resonance.

Table II: Observed Heme Methyl Resonance Shifts (ppm)[a] in Several Heme Proteins

assignments[b]	CcP–N_3	Mb–N_3	Mb–OH	CcP(MI,D235N)
heme 3-CH_3	38.9		31.7	
heme 8-CH_3	36.8	24.4	35.2	33.9
heme 5-CH_3	31.9	31.6	35.2	32.4
heme 1-CH_3	25.8	26.2	25.1	25.8
				19.4

[a] Shifts are reported at various temperatures and conditions: CcP–N_3 = 0.1 M KNO_3, 22 °C, pD = 6.9; Mb–N_3 = 0.1 M phosphate, 25 °C, pD 7.2; Mb–OH = 0.2 M NaCl, 25 °C, pD 11.1; CcP(MI,D235N) = 0.25 M KNO_3, 21 °C, pD = 6.6. Data for sperm whale metmyoglobin are from La Mar et al. (1980). Data for CcP–N_3 are from Satterlee et al. (1983b). [b] Assignments are only for wild-type $CcPN_3$, sperm whale Mb–N_3, and sperm whale Mb–OH. No assignments have yet been made for CcP(MI,D235N).

of this mutant under the conditions presented in Figure 2. These conclusions are consistent with the crystallographically detected movement of the iron ion toward the distal side of the heme in D235N compared to CcP(MI) and the presence of residual density at the heme ligand binding site in the difference map of CcP(MI) vs D235N that suggests a change in axial ligation in D235N (Wang et al., 1990).

(*B*) *Multiple Forms.* The spectra of CcP(MI) (Figure 2B) and D235N (Figure 2C) are both inconsistent with the presence of only single protein forms in solution for these conditions. For CcP(MI), at least one other form is detected from the additional resonances in the spectrum, compared to

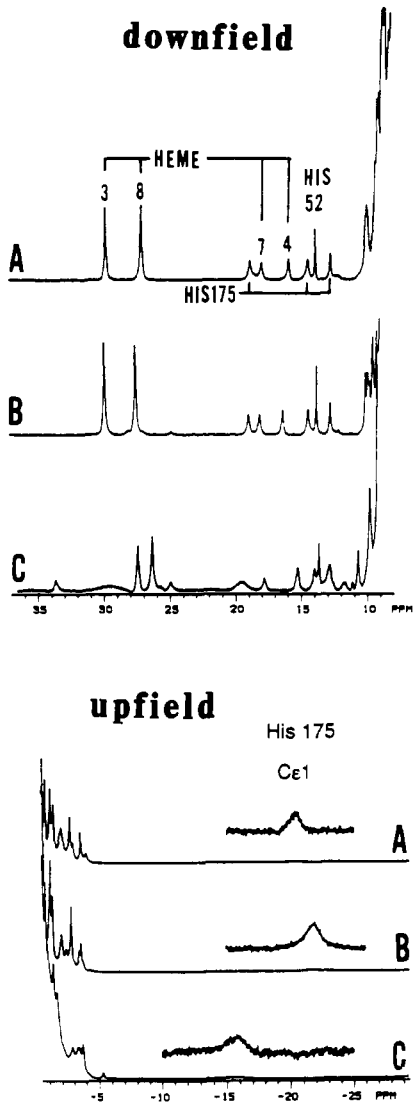

FIGURE 3: 361-MHz proton NMR spectra at 21 °C in the D_2O buffer described in Figure 5: (top) downfield hyperfine resonances of (A) wild-type yeast CcP–CN, (B) CcP(MI)–CN, and (C) D235N–CN; (bottom) upfield hyperfine resonances of (A) wild-type yeast CcP–CN, (B) CcP(MI)–CN, and (C) D235N–CN. Assignments given are those previously made for wild-type yeast CcP–CN.

native CcP. These small peaks occur at 86 ppm and approximately 58 ppm and include the shoulder at approximately 73 ppm. For CcP(MI,D235N) the presence of at least one additional protein form is indicated by the larger-than-expected number of resonances in the downfield hyperfine region. In particular, the smaller resonances at 15.9, 17.7, 29.9, 35.7, and 55.8 ppm, whose integrated areas are nonintegral in relation to the larger peaks, indicate the presence of a minor form or forms. Further indication that at least two spectroscopically detectable protein forms exist in solutions of D235N comes from spectra of the cyanide-ligated proteins shown in Figure 3.

Although low-spin forms will be discussed in detail later, a brief analysis relative to this point is appropriate now. The cyanide-ligated forms of all three proteins are compared in Figure 3, and in these spectra there is further evidence for multiple protein forms for the mutant. Figure 3C [CcP(MI,D235N)–CN] shows that there is a set of smaller resonances (33.6, 29.5, 25.7, 25.0, 13.3, 11.70, and 11.1 ppm) that do not correspond to resonances of CcP–CN or CcP(MI)–CN and whose integrated intensities are not integral factors of the intensities of the larger resonances. These results show that

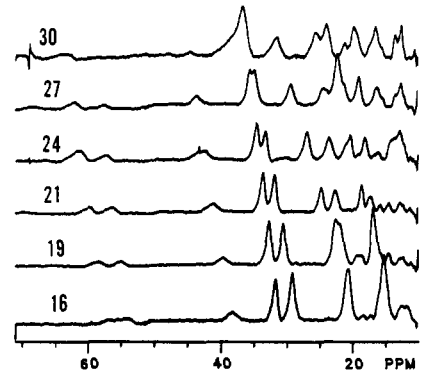

FIGURE 4: Variable temperature dependence of the downfield proton hyperfine shift region of CcP(MI,D235N). Solution conditions are identical with those described for Figure 2.

the spectra of wild-type native CcP (Figure 2A) and wild-type CcP–CN (Figure 3A) display resonance patterns consistent with only single protein forms in each solution. In contrast, for CcP(MI) (Figure 2B), CcP(MI)–CN (Figure 3B), D235N (Figure 2C) and D235N–CN (Figure 3C) at least two protein forms in solutions are detected by proton NMR. Peak integrations carried out on various preparations of both CcP(MI) and D235N (both cyanide ligated and not) allow us to estimate that between 10% and 25% of the protein occurs as the minor form. The variability we have observed in the amount of the minor forms comes both from the uncertainty inherent in deconvoluting and integrating overlapping peaks and from the fact that the amount of minor form depends upon the history of the particular sample and the solution conditions used for NMR spectroscopy. This phenomenon is currently under further investigation. In spite of these spectroscopic indications of solution heterogeneity the mutant protein migrates as a single band on SDS electrophoresis and has been crystallized (Wang et al., 1990), indicating that the spectroscopically distinguishable species may be interconverting forms of the same protein in solution.

(*C*) *Spin-State Equilibrium.* A previous study of CcP(MI,D235N) utilizing resonance Raman spectroscopy provided evidence for the presence of a spin-state equilibrium (Smulevich et al., 1988). We can support this conclusion for D235N on the basis of variable-temperature proton NMR experiments, examples of which are shown in Figure 4. The downfield hyperfine resonances (Figure 4) exhibit increasing shift magnitudes (downfield shifts) with increasing temperature, above 14 °C. This is "anti-Curie" behavior in the sense that normal Curie law behavior predicts upfield shifts with increasing temperature (Satterlee, 1986). Curie plots of our extensive variable temperature experiments of D235N further illustrate the anti-Curie phenomenon (data not shown). The anti-Curie behavior observed for D235N (Figure 4) is consistent with the existence of a solution-state dynamic equilibrium involving a temperature-dependent population of a thermally accessible excited state.

For a paramagnetic system such as this, the anti-Curie behavior of CcP(MI,D235N) is most likely caused by a spin-state equilibrium that is facilitated by heme axial ligation changes. We infer this from the following. The low-temperature form displays smaller shifts and normal Curie behavior below 14 °C (data not shown) that is characteristic of a low-spin ferriheme protein. Above 14 °C, the anti-Curie behavior displayed in Figure 4 indicates that the protein dynamically interconverts with another form. The nature of the anti-Curie behavior shown in Figure 4 requires that this other form exhibit large downfield shifts and broader resonances,

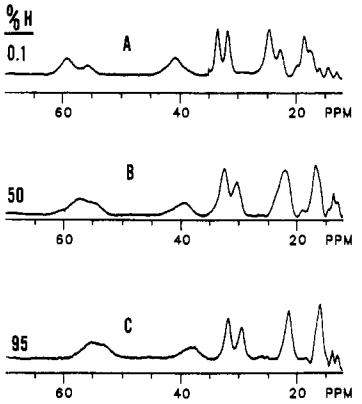

FIGURE 5: Effect of changing solvent composition on CcP(MI,D235N) downfield proton hyperfine shifts (361 MHz). Percent protium (H) of the solvent is indicated at the left of each spectrum (21 °C, 0.15 M KNO_3, 0.05 M potassium phosphate). (A) 99.9% D_2O, pD = 6.8; (B) 50% D_2O/50% H_2O, meter reading 6.9; (C) 95% H_2O, pH = 7.1.

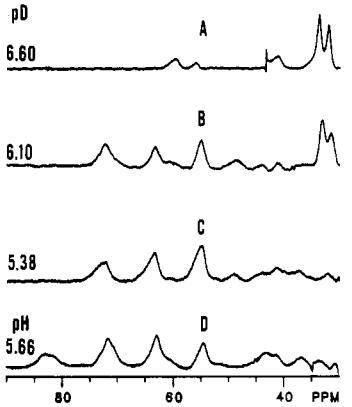

FIGURE 6: Proton NMR spectra (361 MHz) of the downfield hyperfine shift region for CcP(MI,D235N) showing the effect of changing pD in 99.9% D_2O buffer solutions (A–C). The effect of changing solvent composition at low pH is illustrated by the proton spectrum of the same region for D235N in 95% H_2O buffer solution in (D). Buffer in (A–C) is identical with that described for Figure 5.

such as those displayed by high-spin forms like wild-type native CcP and CcP(MI) (Figure 2A,B).

On the basis of this reasoning and pD dependence data presented later, we interpret these results for D235N as indicating interconversion between low- and high-spin heme protein forms. The data show that the high-spin form is progressively populated with increasing temperature, thereby accounting for the behavior shown in Figure 4. At the high-temperature limit of this experiment (38 °C), which was also at the limit of the protein's stability, resonances disappeared from the downfield hyperfine shift region presumably as a result of extreme exchange broadening and protein denaturation.

(*D*) *Occupation of the Ligand Binding Site.* Information on the occupation of the heme ligand binding site in the mutant comes from solvent exchange studies. For D235N, the hyperfine shift pattern depends upon whether or not the protein is in D_2O or H_2O, as shown in Figure 5. At pH 6.8 and 21 °C, D235N is predominantly low spin, as demonstrated by the small downfield hyperfine shift range. The solvent effect (Figure 5) does not alter this situation because similarly small hyperfine shifts for D235N are observed in both solvents. However, the precise pattern of shifts is different in each solvent. This solvent isotope effect has also been reported for native (yeast) CcP preparations in this same buffer (La Mar et al., 1988) that demonstrated "nonaged" (Smulevich et al., 1989; Yonetani & Anni, 1987) spectroscopic characteristics.

The previous results were interpreted as solvent-induced alteration of the heme iron's axial ligand field. In that case, water was implicated as a sixth heme ligand in the "nonaged" form of wild-type CcP, and it was considered to be the source of the solvent isotope effect. The relatively large hyperfine shift dependence upon the solvent composition (H_2O vs D_2O) shown in Figure 5 is consistent with solvent involvement at the heme ligand binding site in the mutant protein, as well. However, since a water molecule is a weak-field ligand, its presence in the heme's sixth coordination position would be insufficient to create a low-spin heme. Hydroxide as the sixth heme ligand, however, would be consistent with *both* formation of a low-spin heme and the demonstrated solvent isotope sensitivity, with both OH^- and OD^- capable of coordinating to the heme, but with each exerting slightly different axial ligand field strengths. The different axial ligand field strengths, however minor, are enough to modify the bonding within the heme prosthetic group, resulting in altered patterns of unpaired spin density delocalization. This effect ultimately manifests itself in a display of slightly different hyperfine shift patterns.

(*E*) *pH Dependence.* Lowering the pH (pD) of a D_2O solution of D235N to pD 5.38 (Figure 6) transforms its spectrum into one that is comparable to the spectra of wild-type native CcP and CcP(MI) at pD 6.8, both of which are typical of high-spin ferriheme proteins. This is shown by comparing the low-pH spectrum (pD 5.38) of D235N in Figure 6C with the spectra of wild-type CcP and CcP(MI) shown in Figure 2A,B. The low-pH spectrum of D235N (Figure 6C) displays three major resonances at 72.1, 63.2, and 54.9 ppm (21 °C, pD = 5.38) and some broad, less intense resonances between 30 and 50 ppm. The pattern of relatively more intense resonances downfield from 50 ppm and smaller resonances between 30 and 60 ppm is similar to that displayed by wild-type CcP and CcP(MI) at pD 6.8 (Figure 2A,B). As indicated in Figure 2, the more intense resonances for wild-type CcP are assigned to the four heme methyl substituents. The pD 5.38 spectrum of D235N in D_2O (Figure 6C) is unusual in that only three resonances are detected which are of appropriate relative intensity and shift to be assigned to the heme methyl substituents. However, in H_2O solutions (Figure 6D) four major heme methyl resonances are detected in the spectrum of D235N. That spectrum is more reminiscent of the wild-type CcP and CcP(MI) high-spin-type spectra in Figure 2. In D_2O the resonances of D235N at low pD are quite broad, with line widths varying between 800 and 1300 Hz. Consequently, their shapes are hard to define and it is possible that the fourth methyl resonance is degenerate with one of the other resonances or that it is so broad that it went undetected.

The transformation shown in Figure 6 is characteristic of a pH-dependent axial ligation and spin-state change at the heme. The results shown in Figure 6 are consistent with a transition between hydroxo- (low-spin) and (high-spin) aquo–heme ligation, such as that depicted schematically in Figure 7. Apparently, the effect of this proximal-side mutation is to alter the p*K* for a distal-side heme ligand, in this case a water molecule. In native wild-type CcP this acid/alkaline transition is normally observed above pH 8.

The low-pH spectrum of D235N also exhibits a solvent isotope effect (Figure 6C,D) that is more dramatic than that demonstrated by wild-type native CcP (La Mar et al., 1988). In 90% H_2O/10% D_2O the spectrum is remarkably similar to those exhibited by wild-type native CcP and CcP(MI) (Figure 2A,B). There are four detectable downfield heme

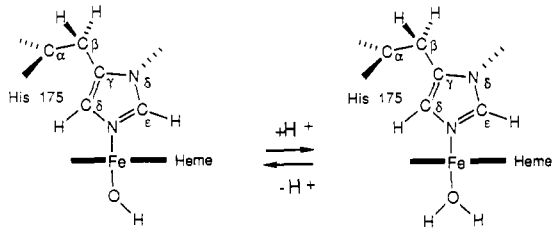

FIGURE 7: Schematic representation of the aquo/hydroxo ligation equilibrium for CcP(MI,D235N) that is inferred from the NMR pH titration data (Figure 6).

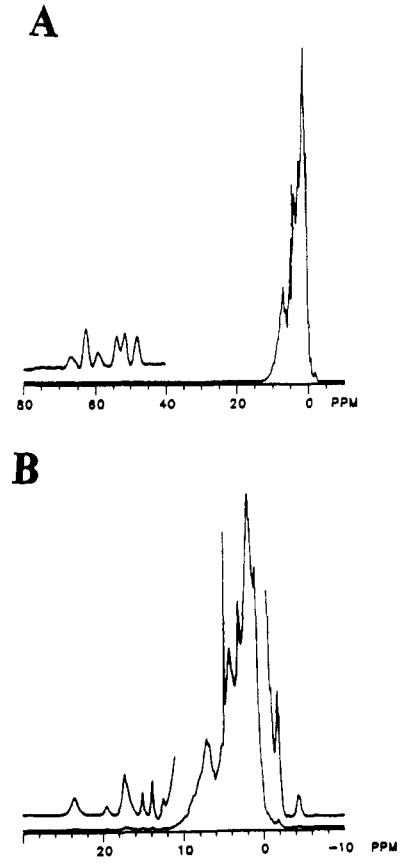

FIGURE 8: 361-MHz proton NMR spectra of (A) fluoride-ligated CcP(MI,D235N) at 25 °C in the D_2O buffer described in Figure 5 at pD 5.53 and (B) azide-ligated CcP(MI,D235N) at pD 6.3 in the D_2O buffer described in Figure 5.

methyl resonances (peaks centered at 83.1, 71.5, 62.8, and 54.5 ppm; 21 °C, pH = 5.66), and because of this, the spectrum can be taken to represent high-spin CcP(MI,D235N). This result further indicates that, at low pH, a molecule of water occupies the sixth heme coordination site of D235N in close enough proximity to the heme iron ion to affect its axial ligand field via a solvent effect, as discussed above.

Ligated Proteins. (A) Fluoride Ion Ligation. CcP(MI,-D235N) binds potassium fluoride to yield a proton spectrum (Figure 8A) that is similar to that of wild-type CcP–F (Satterlee et al., 1983a), with four major resonances occurring between 48 and 65 ppm. In wild-type CcP–F, the major resonances in this region have been assigned to the four heme methyl protons (Satterlee et al., 1983a). In D235N–F, the major resonances also are presumably due to the heme methyls. These resonances occur at 62.8, 54.1, 51.8, and 48.2. ppm (25 °C, pD = 5.53). One functional difference between wild-type CcP and the mutant protein is that bound fluoride ion can be removed from wild-type CcP by dialysis, whereas extensive dialysis of D235N–F over 4 days, against several

Table III: Observed Resonance Shifts (ppm) for Cyanide-Ligated Proteins[a]

assignments[b]	CcP–CN[c]	CcP(MI)–CN	CcP(MI,-D235N)–CN
			33.60
			27.5–31 br
heme 3-CH_3	30.66	30.56	27.38
heme 8-CH_3	27.59	27.99	26.28
			25.66
			25.0
His-175 $C_\beta H$	19.39	19.42	19.50
heme 7α	18.21	18.32	17.70
heme 4α	15.92	16.36	15.16
His-175 $C_\beta H$	14.78	14.67	13.89
His-52 $C_{\epsilon 1}$	14.00	13.88	13.57
His-175 Np	12.85	12.86	12.75
			11.70
			11.05
			10.64
	−1.21	−1.18	
heme 7β	−1.51	−1.39	−1.36
			−1.68
heme 4βtrans	−2.23	−2.24	
	−2.86	−2.98	−2.98
	−3.27		−3.39
			−3.53
heme 4βcis	−3.94	−3.92	−3.83
	−4.59		
			−5.43
His-175 $C_{\epsilon 1}$	−20.77	−22.43	−15.75

[a] Protein concentration = 1.8–2.4 mM; 260 mM KNO_3, 40 mM phosphate buffer, pD 6.9 ± 0.1, 21 ± 1 °C; shifts, in ppm, reported relative to internal HDO = 4.63 ppm. [b] Firm assignments have only been made for wild-type CcP–CN (Satterlee et al., 1983b); consistent assignments for the other two proteins are inferred from the similarity in corresponding shift positions. [c] Wild type.

thousand-fold volume changes of buffer solutions, produced no noticeable change in the proton spectrum. This result indicates that the dynamics of fluoride binding by the mutant protein are different from those of wild-type CcP. This is another indication that the point mutation in D235N results in modified chemical properties at the heme ligand binding site. It is possible to replace fluoride ion as a heme ligand by cyanide ion and azide ion, both of which are stronger field ligands than fluoride ion. The resonances of D235N–F exhibit normal Curie temperature dependence (data not shown).

(B) Low-Spin Forms: Azide and Cyanide Ligation. Similar to wild-type native CcP and CcP(MI), both KCN and NaN_3 convert D235N to low-spin forms, as shown in Figures 3 and 8B. These low-spin forms are characterized by resonances with narrower line widths and smaller downfield isotropic shifts than either the low-pH or fluoride-ligated forms of D235N discussed above. For D235N–N_3, the spectrum in Figure 8B is generally similar to that of wild-type CcP–N_3 (Satterlee et al., 1983b), but different enough so as not to be directly comparable in the absence of resonance assignments, so no further analysis is warranted until assignments for D235N–N_3 are available.

The full proton spectrum of CcP(MI)–CN is virtually identical with that of wild-type CcP–CN (Satterlee et al., 1983b), particularly in the 0–10 ppm region (data not shown). A comparison of the downfield hyperfine shift region for wild-type CcP–CN, CcP(MI)–CN, and D235N–CN is given in Figure 3. Comparing the spectra in the top portion of Figure 3 (Figure 3A,B) reveals that between 35 and 11 ppm the spectra of wild-type CcP–CN and CcP(MI)–CN contain identical numbers of resonances that demonstrate similar shifts. Despite minor shift differences (Table III), the correspondence in downfield hyperfine resonance patterns of CcP(MI)–CN and wild-type CcP–CN allows us to conclude that the assignments made for wild-type CcP–CN (Satterlee et al., 1983b, 1987) are directly applicable to CcP(MI)–CN (Figure

3 and Table III). This correspondence means that the immediate heme environments of the two proteins in solution are quite similar, as expected from the crystal structures (Wang et al., 1990).

In contrast to the essentially identical downfield hyperfine shift regions for wild-type CcP–CN and CcP(MI)–CN, the spectrum of D235N–CN (Figure 3C, top) reveals a set of resonances in which nearly all of the downfield isotropic resonances are shifted upfield relative to the resonances in spectra of wild-type CcP–CN and CcP(MI)–CN (Table III). The effect is largest for the heme peripheral substituents, such as the 8-methyl and 3-methyl resonances. Despite this upfield bias there is some correlation in the overall hyperfine resonance patterns of D235N–CN with wild-type CcP–CN and CcP(MI)–CN that is revealed in Figure 3. Reasonable corresponding assignments for D235N–CN that are based on spectral pattern similarities with wild-type CcP–CN are given in Table III.

What could be the origin of the significant shift differences demonstrated for D235N–CN in Figure 3? The isotropic shift for a proton in wild-type CcP–CN is due to both contact and dipolar contributions (Satterlee, 1986). If mutation has resulted in a change in magnetic anisotropy, then a change in the dipolar shift is responsible for the observed isotropic shift differences for the mutant. We do not believe this to be the case since we have identified two wild-type CcP–CN resonances that are due to protons so remote from the heme that their shifts are wholly dipolar. These are His-52 ϵ_1H and His-175 peptide NH. Although physically remote from the heme site both protons exhibit temperature dependence (Satterlee & Erman, 1983). As shown in Table III and Figure 3 (top), only minor shift changes are observed for these protons in the three proteins, evidence that no major net difference in dipolar shift and magnetic anisotropy occurs between these three proteins.

Without knowing the precise positions and assignments for all of the heme pyrrole substituent protons, it is difficult to absolutely rule out changes in magnetic anisotropy as the cause of the observed isotropic shift differences found for D235N–CN. However, the evidence so far suggests no major difference in magnetic anisotropy between wild-type CcP–CN, CcP(MI)–CN, and D235N–CN. Since the isotropic shifts of heme pyrrole substituents are dominated by contact shifts due to unpaired spin density delocalized in heme 3eπ orbitals (La Mar, 1979; La Mar & Walker, 1979), it seems more likely that the isotropic shift changes seen in Table III for D235N–CN compared to Ccp(MI)–CN are a result of changes in the pattern for π-type unpaired spin density delocalization. The data in Table III reveal that the mutation-induced shifts for the heme pyrrole II and IV substituents are the largest and they are all upfield, suggesting a decrease in assymmetry of the heme 3eπ orbital unpaired spin density. For the mutant D235N–CN this is probably brought about by changes in proximal-side heme contacts, which involve changes in inductive effects, most likely caused by reorientation of the protein on the proximal side (Wang et al., 1990), as well as changes in His-175–Fe–heme bonding caused by a significant change in His-175 protonation state (vide infra). In ferric heme model systems both of these types of interactions were found to be capable of altering porphyrin unpaired spin density distributions (La Mar et al., 1978; Goff, 1980; Traylor & Berzinis, 1980; Walker, 1980).

Another difference between the proton NMR spectra of D235N–CN, on the one hand, and wild-type CcP–CN and CcP(MI)–CN, on the other, is the observation of small resonances at 33.6, 29.5, 25.7, 25.0, 11.05, and 11.7 ppm in the D235N–CN spectrum. For reasons described earlier, these indicate the existence of at least one additional form of CcP(MI,D235N)–CN in solution. The resonance near 34 ppm in the minor form exhibits strong magnetization transfer from the resonance near 27.4 ppm in the major form (data not shown), indicating that these two peaks probably correspond to the same methyl group in the different enzyme forms.

(*C*) *Histidine 175 Protonation Status.* A comparison of the upfield shift regions for all three cyanide-ligated proteins is shown in Figure 3 (bottom). There are obvious differences in the 0 to −6 ppm region, although, again, the spectra of wild-type CcP–CN (Figure 3A, bottom) and CcP(MI)–CN (Figure 3B, bottom) are very similar in this region. In contrast, the mutant D235N–CN exhibits significant differences between 0 and −6 ppm.

Further upfield in each spectrum is the broad single proton resonance that, on the basis of studies of both model systems and other ferriheme proteins, has been assigned to the heme-coordinated histidine (Satterlee & La Mar, 1976; La Mar et al., 1976, 1982). For wild-type native CcP it is His-175 $C_{\epsilon 1}$H (Figure 1). Previous studies (La Mar et al., 1982) have shown that, for a series of model compounds, the relative shifts of ferriheme-coordinated histidine or imidazole $C_\beta H_2$ and $C_{\epsilon 1}$H resonances correlate with the degree of charge carried by the imidazole or histidine. That work revealed that larger shifts of the His-175 $C_{\epsilon 1}$ and C_β protons (i.e., resonances lying further from 0 ppm) occur for heme-coordinated histidine *imidazolate* rings (Figure 1C), whereas smaller shifts of these protons (i.e., resonances lying closer to 0 ppm) occur for *neutral* heme-coordinated histidine imidazole rings (Figure 1B). From Table III and Figure 3, it is obvious that the mutant protein D235N–CN exhibits the smallest His-175 $C_{\epsilon 1}$ and C_β proton shifts, which means that, contrasted with wild-type CcP–CN and CcP(MI)–CN, D235N–CN possesses a more neutral His-175 imidazole ring (Figure 1B). The wild-type CcP–CN and CcP(MI)–CN spectra each represent proteins in which His-175 exhibits significant imidazolate character (represented schematically in either Figure 1A or Figure 1C). This result confirms the expectation that the Asn substitution of Asp-235 in the mutant protein has altered proximal-side hydrogen bonding so that His-175 exists in a protonated, or relatively more protonated, form than in the parent enzyme.

Summary

This work demonstrates that introducing an Asp-235 → Asn mutation into CcP alters the properties of the heme in several ways. *First*, it alters the proximal hydrogen bond network so that the D235N–CN mutant protein displays spectroscopic properties characteristic of a more neutral proximal histidine, rather than the more negatively charged (imidazolate) proximal histidines of wild-type CcP–CN and CcP(MI)–CN. *Second*, it changes the ligand binding properties of the protein. CcP(MI,D235N) displays an altered pK for water localized in the ligand binding pocket so that at neutral pH D235N is low-spin and hydroxy-ligated. *Third*, the mutant protein, D235N, displays relatively tighter binding of fluoride ion. *Fourth*, the cyanide-ligated mutant protein D235N–CN displays altered proton NMR spectra, reflecting changes in the heme unpaired spin density distribution brought about by disruption of the His-175–Asp-235 hydrogen bond that occurs in wild-type CcP–CN and Ccp(MI)–CN.

The NMR results presented here establish the existence of a substantial His-175–Asp-235 hydrogen bond in wild-type CcP–CN and CcP(MI)–CN, with concomitant formation of a more negative heme coordinated His-175 relative to the

D235N mutant. It is likely that a completely deprotonated imidazole ring of His-175 occurs in the low-spin forms of wild-type CcP, just as demonstrated for HRP–CN. The NMR data of Figure 3 definitely suggest this to be the case. However, our inability to detect the His-175 N_δ proton in wild-type native CcP (due to CcP's lower temperature stability compared to HRP) makes this latter point inconclusive. Furthermore, on the basis of our identification of asymmetric hydrogen bonding, or complete proton transfer from His-175 in CcP–CN and CcP(MI)–CN, it is likely that this also occurs in high-spin, unligated wild-type CcP and CcP(MI) and their ferryl enzyme intermediates.

Registry No. CcP, 9029-53-2; L-Asp, 56-84-8; L-Asn, 70-47-3; L-His, 71-00-1; F^-, 16984-48-8; N_3^-, 14343-69-2; CN^-, 57-12-5; heme, 14875-96-8.

References

Blumberg, W. E., & Peisach, J. (1971) in *Probes of Structure and Function of Macromolecules and Membranes* (Chance, B., Yonetani, T., & Mildvan, A., Eds.) Vol. II, pp 533–543, Academic Press, New York.

de Ropp, J. S., Thanabal, V., & La Mar, G. N. (1985) *J. Am. Chem. Soc. 107*, 8268–8270.

Finzel, B. C., Poulos, T. L., & Kraut, J. (1984) *J. Biol. Chem. 259*, 13027–13036.

Fishel, L. A., Villafranca, J. E., Mauro, J. M., & Kraut, J. (1987) *Biochemistry 26*, 351–360.

Goff, H. (1980) *J. Am. Chem. Soc. 102*, 3252–3254.

Krishnamoorthi, R., La Mar, G. N., Mizukami, H., & Romero, A. (1984) *J. Biol. Chem. 259*, 265–270.

La Mar, G. N. (1979) in *Biological Applications of Magnetic Resonance* (Shulman, R. G., Ed.) pp 305–344, Academic Press, New York.

La Mar, G. N., & Walker, F. A. (1979) in *The Porphyrins* (Dolphin, D., Ed.) Vol. IV, pp 61–155, Academic Press, New York.

La Mar, G. N., Frye, J. S., & Satterlee, J. D. (1976) *Biochim. Biophys. Acta 428*, 78–90.

La Mar, G. N., Viscio, D. B., Smith, K. M., Caughey, W. S., & Smith, M. L. (1978) *J. Am. Chem. Soc. 100*, 8085–8092.

La Mar, G. N., Budd, D. L., & Smith, K. M. (1980) *Biochim. Biophys. Acta 622*, 210–218.

La Mar, G. N., de Ropp, J. S., Chacko, V. P., Satterlee, J. D., & Erman, J. E. (1982) *Biochim. Biophys. Acta 708*, 317–325.

McGrath, T. M., & La Mar, G. N. (1978) *Biochim. Biophys. Acta 534*, 99–111.

Mincey, T., & Traylor, T. G. (1979) *J. Am. Chem. Soc. 101*, 765–770.

Morrison, M., & Schonbaum, G. R. (1976) *Annu. Rev. Biochem. 45*, 861–888.

Peisach, J. (1975) *Ann. N.Y. Acad. Sci. 244*, 187–200.

Poulos, T. L., & Kraut, J. (1980) *J. Biol. Chem. 255*, 8199–8205.

Satterlee, J. D. (1986) in *Annual Reports on NMR Spectroscopy* (Webb, G. A., Ed.) Vol. 17, pp 79–178, Academic Press, London.

Satterlee, J. D., & La Mar, G. N. (1976) *J. Am. Chem. Soc. 98*, 2804–2808.

Satterlee, J. D., & Erman, J. E. (1980) *Arch. Biochem. Biophys. 202*, 608–616.

Satterlee, J. D., & Erman, J. E. (1983) *J. Biol. Chem. 258*, 1050–1056.

Satterlee, J. D., Erman, J. E., La Mar, G. N., Smith, K. M., & Langry, K. C. (1983a) *Biochim. Biophys. Acta 743*, 246–255.

Satterlee, J. D., Erman, J. E., La Mar, G. N., Smith, K. M., & Langry, K. C. (1983b) *J. Am. Chem. Soc. 105*, 2099–2104.

Satterlee, J. D., Erman, J. E., & de Ropp, J. S. (1987) *J. Biol. Chem. 262*, 11578–11583.

Smulevich, G., Mauro, J. M., Fishel, L. A., English, A. M., Kraut, J., & Spiro, T. G. (1988) *Biochemistry 27*, 5477–5485.

Smulevich, G., Mantini, A. R., English, A. M., & Mauro, J. M. (1989) *Biochemistry 28*, 5058–5064.

Traylor, T. G., & Berzinis, A. P. (1980) *J. Am. Chem. Soc. 102*, 2844–2846.

Traylor, T. G., & Popovitz-Biro, R. (1988) *J. Am. Chem. Soc. 110*, 239–243.

Walker, F. A. (1980) *J. Am. Chem. Soc. 102*, 3254–3256.

Walker, F. A., Lo, M. W., & Ree, M. T. (1976) *J. Am. Chem. Soc. 98*, 5552–5554.

Walker, F. A., Buehler, J., West, J. T., & Hinds, J. L. (1983) *J. Am. Chem. Soc. 105*, 6923–6929.

Wang, J., Mauro, J. M., Edwards, S. L., Oatley, S. J., Fishel, L. A., Ashford, V. A., Xuong, N., & Kraut, J. (1990) *Biochemistry 29*, 7160–7173.

Yonetani, T., & Anni, H. (1987) *J. Biol. Chem. 262*, 9547–9554.